Fuertes-Miquel, VS.; Coronado-Hernández, OE.; Iglesias Rey, PL.; Mora Melia, D. (2019). Transient phenomena during the emptying process of a single pipe with water air interaction. Journal of Hydraulic Research. 57(3):318-326. https://doi.org/10.1080/00221686.2018.1492465

To appear in the *Journal of Hydraulic Research*
Vol. 00, No. 00, Month 20XX, 1–22

Research paper

# Transient phenomena during the emptying process of a single pipe with water-air interaction

VICENTE S. FUERTES-MIQUEL (IAHR Member), Associate Professor, *Departamento de Ingeniería Hidráulica y Medio Ambiente, Universitat Politècnica de València, Valencia, Spain*
*Email: vfuertes@upv.es (author for correspondence)*

OSCAR E. CORONADO-HERNÁNDEZ, PhD Student, *Departamento de Ingeniería Hidráulica y Medio Ambiente, Universitat Politècnica de València, Valencia, Spain;* Assistant Professor*, Facultad de Ingeniería, Universidad Tecnológica de Bolívar, Cartagena, Colombia*
*Email: ocoronado@utb.edu.co*

PEDRO L. IGLESIAS-REY, Associate Professor, *Departamento de Ingeniería Hidráulica y Medio Ambiente, Universitat Politècnica de València, Valencia, Spain*
*Email: piglesia@upv.es*

DANIEL MORA-MELIÁ, Assistant Professor, *Departamento de Ingeniería y Gestión de la Construcción, Universidad de Talca, Curicó, Chile*
*Email: damora@utalca.cl*

*Running Head:* the emptying process of a single pipe.

v1.0 released April 2015

Transient phenomena during the emptying process of a single pipe with water-air interaction

**ABSTRACT**
Emptying pipelines can be critical in many water distribution networks because subatmospheric pressure troughs could cause considerable damage to the system due to the expansion of entrapped air. Researchers have given relatively little attention to emptying processes compared to filling processes. The intricacy of computations of this phenomenon makes it difficult to predict the behavior during emptying, and there are only a few reliable models in the literature. In this work, a computational model for simulating the transient phenomena in single pipes is proposed, which was validated using experimental results. The proposed model is based on a rigid column to analyze water movement, the air-water interface, and air pocket equations. Two practical cases were used to validate the model: 1) a single pipe with the upstream end closed, and 2) a single pipe with an air valve installed on the upstream end. The results show how the model accurately predicts the experimental data, including the pressure oscillation patterns and subatmospheric pressure troughs.

*Keywords:* Air-water, air valve, entrapped air, pipelines emptying, transient flow, water distribution networks.

## 1 Introduction

Over recent decades, the analysis of transient phenomena for a single-phase liquid has been studied extensively by researchers and there are currently numerous models that represent correctly the water behavior in any hydraulic system. However, transient flow with trapped air is much more complex to simulate because there are two fluids (water and air) in two different phases (liquid and gas) (Fuertes, 2001), which implies a higher complexity to establish reliable mathematical models.

Filling and emptying maneuvers are common pipelines operations with trapped air. These operations are repeated periodically and must be considered to avoid future problems associated to extreme values of air pocket pressure. For this reason, many researchers have focused their efforts on the development of different models for the analysis on entrapped air in water supply networks (Coronado-Hernández, Fuertes-Miquel, Iglesis-Rey, & Martínez-Solano, 2018; Martins, Ramos, & Almeida, 2015; H. Wang et al., 2016; Zhou, Liu, & Karney, 2013a).

To date, researchers have mostly focused on filling processes, developing models that have shown great accuracy in comparison to experimental data. In this sense, early studies on pipelines were conducted by Liou and Hunt (1996) and Izquierdo, Fuertes, Cabrera, Iglesias, and Garcia-Serra (1999), and Zhou et al. (2013a); Zhou, Liu, and Karney (2013b) developed recently models to analyze the process of rapid filling. Additionally, a few pieces of research have been published analyzing the influence of different parameters through experimental investigations of the systems (Hou et al., 2014; Zhou & Liu, 2013).Finally, others studies have focused on techniques and methods for solving the filling problem (Liu, Zhou, Karney, Zhang, & Ou, 2011; Malekpour & Karney, 2014; Martins, Ramos, & Almeida, 2010; Martins et al., 2015; H. Wang et al., 2016), analyzing the consequences of the formation of air pockets (Pozos, González, Giesecke, Marx, & Rodal, 2010), and the occurrence of cavitation in the propagation of transient phenomena (Bashiri-Atrabi & Hosoda, 2015; Guinot, 2001; K. Wang, Shen, & Zhang, 2003).

Emptying processes may also be critical, but they have received less attention from researchers. On this matter, Laanearu et al. (2012) developed a semi-empirical model for estimating local energy losses and Tijsseling, Hou, Bozkuş, and Laanearu (2016) presented a model for the emptying process with pressurized air in a pipeline. Nevertheless, there is a lack of studies on the water draining maneuvers in engineering applications of real hydraulic systems.

Therefore, this paper presents a new mathematical model to be used for emptying processes. The proposed model simulates the liquid column with a rigid model using the mass oscillation equation (Cabrera, Abreu, Pérez, & Vela, 1992; Izquierdo et al., 1999; Lee, 2005; Liou & Hunt, 1996), which provides sufficient accuracy by using a moving air-water interface (Izquierdo et al., 1999; Zhou et al., 2013a). Additionally, it is possible to consider thermodynamic behaviors such as: (a) an isothermal process, where the temperature remains constant inside the hydraulic installation; (b)

an adiabatic process, where the hydraulic installation exchanges no heat with its surroundings; and (c) an intermediate processes, which involves temperature change and heat transfer. In this sense, the relationship between the absolute pressure and total volume of entrapped air characterizes the behavior of air, which is known as a polytropic process. If the transient process occurs slowly enough, it is considered isothermal, and the polytrophic coefficient is 1.0. In contrast, if the transient process is fast enough, it is considered adiabatic, and the polytrophic coefficient is 1.4 (Fuertes-Miquel, López-Jiménez, Martínez-Solano, & López-Patiño, 2016; Izquierdo et al., 1999; Martin, 1976; Martins et al., 2015; Zhou et al., 2013b). In actual installations, isothermal or adiabatic processes are rare, so an intermediate situation occurs.

This work applies the developed model to the emptying process in two cases. On one hand, Case No. 1 corresponds to a single pipe with the upstream end closed without an air valve. As such, it is not possible to empty the pipeline, so subatmospheric pressure troughs are generated and may collapse the system. In this case, a polytrophic evolution of the air pocket is used (Zhou et al., 2013b). On the other hand, Case No. 2 corresponds to a single pipe with an air valve installed on the upstream end, which protects the system during the emptying process. As there is air inlet, this case also needs the continuity equation of the air pocket, the expansion-compression equation of the entrapped air pocket (Leon, Ghidaoui, Schmidt, & Garcia, 2010; Martin, 1976), and the air valve characterization (Iglesias-Rey, Fuertes-Miquel, García-Mares, & Martínez-Solano, 2014; Wylie & Streeter, 1993). Water column separation cannot be predicted by this model, but such a situation rarely occurs in normal water emptying processes. In each case, systems of differential-algebraic equations (DAE) are solved using numerical methods. Computational simulations were performed using the Simulink Library in Matlab. The proposed model was validated by comparing the computed pressure oscillation patterns with measured results. This study shows how the model fits the experimental data, and the results can be used to develop practical applications for emptying processes.

## 2 Mathematical model

This section presents a mathematical model to analyze the emptying process in a single pipe. Figure 1 shows the configurations for the two cases analyzed.

### 2.1 *Case No. 1: A simple pipe with the upstream end closed*

The emptying process in a simple pipe with the upstream end closed contains an air pocket inside the installation (see Fig. 1a).

The following assumptions were made for the analysis:

- The water behavior is modeled with the rigid model approach.
- The slope, diameter, and pipe roughness are considered constant
- A constant friction factor accounts for losses using the Darcy-Weisbach equation (Izquierdo et al., 1999; Laanearu et al., 2012; Liou & Hunt, 1996; Tijsseling et al., 2016; Zhou et al., 2013a).
- A polytrophic coefficient is used to model the behavior of entrapped air.
- A valve is installed on the downstream end.
- The air-water interface is a well-defined cross section and can be applied for single pipes (for small diameters or hydraulic slopes so that free-surface flow does not arise) (Liou & Hunt, 1996).
- The pipe can resist dangerous troughs of subatmospheric pressure during transient phenomena.

Under these hypotheses, the problem is modeled as follows:

*Emptying column*

- The mass oscillation equation for an emptying column (rigid column approach) is (Fuertes, 2001):

$$\frac{dv_w}{dt} = \frac{p_1^* - p_{atm}^*}{\rho_w L_e} + g\frac{\Delta z_1}{L_e} - f\frac{v_w|v_w|}{2D} - \frac{R_v g A^2 v_w|v_w|}{L_e} \tag{1}$$

  where $v_w$ = water velocity, $p_1^*$ = absolute pressure of air pocket, $p_{atm}^*$ = atmospheric pressure, $\rho_w$ = water density, $L_e$ = length of emptying column, $\Delta z_1$ = elevation difference, $g$ = gravity acceleration, $f$ = Darcy-Weisbach friction factor, $D$ = internal pipe diameter, $A$ = cross sectional area of pipe, $R_v$ = resistance coefficient, and $Q_w$ = water discharge. Minor losses in the valve are estimated using the formulation $h_m = R_v Q_w^2$.
- The interface position of the emptying column is represented as:

$$\frac{dL_e}{dt} = -v_w \quad \left(L_e = L_{e,0} - \int_0^t v_w \mathrm{d}t\right) \tag{2}$$

  where $L_{e,0}$ = initial value of $L_e$.

*Air pocket*

- The entrapped air pocket is represented by:

$$p_1^* V_a^k = p_{1,0}^* V_{a,0}^k \quad or \quad p_1^* x^k = p_{1,0}^* x_0^k \tag{3}$$

  where $V_a$ = air volume, $V_{a,0}$ = initial air volume, $p_{1,0}^*$ = initial value of $p_1^*$, $k$ = polytropic coefficient, $x$ = length of entrapped air pocket, and $x_0$ = initial length of $x$.

In summary, a 3x3 system of DAE (equations (1)-(3)) describes the problem. The DAE with the corresponding boundary and initial conditions, can be solved for 3 unknowns ($v_w$, $L_e$, and $p_1^*$).

*Initial and boundary conditions*

Initially, the system is considered at rest ($t = 0$). Then, the initial conditions are described by $v_w(0) = 0$, $L_{e,0} = L_T - x_0$, and $p_{1,0}^* = p_{atm}^* = 101325$ Pa.

The upstream boundary condition is given by $p_{1,0}^*$ (initial condition of air pocket), and the downstream boundary condition is given by $p_{atm}^*$ (water free discharge to the atmosphere).

*Gravity term*

The gravity term ($\Delta z_1/L_e$) in equation (1) is constant and can be modeled by this equation:

$$\frac{\Delta z_1}{L_e} = \sin(\theta) \tag{4}$$

### 2.2 *Case No. 2: A simple pipe with an air valve installed in the upstream end*

Figure 1b shows the analyses of the emptying process in a simple pipe with an air valve at the upstream end. The assumptions are the same as in Case No. 1. Equation (1) and equation (2) represent the emptying of the water column. The air pocket is modeled with these equations:

- Continuity equation: This equation is used, considering that the air density of the air pocket ($\rho_a$) and the air density inside the air valve ($\rho_{a,nc}$) involve different properties (see Fig. 2).
  Applying the continuity equation:

$$\frac{dm_a}{dt} = \rho_{a,nc} v_{a,nc} A_{adm} \tag{5}$$

  and deriving the expression:

$$\frac{dm_a}{dt} = \frac{d(\rho_a V_a)}{dt} = \frac{d\rho_a}{dt} V_a + \frac{dV_a}{dt} \rho_a \tag{6}$$

  where $m_a$ = air mass, $v_{a,nc}$ = air velocity in normal conditions admitted by the air valve, and $A_{adm}$ = cross sectional area of the air valve.
  If $V_a = xA = (L_T - L_e)A$ and $dV_a/dt = -(dL_e/dt)A = vA$, then:

$$\frac{d\rho_a}{dt} = \frac{\rho_{a,nc} v_{a,nc} A_{adm} - v_w A \rho_a}{A(L_T - L_e)} \tag{7}$$

- Expansion-compression equation (Lee, 2005; Leon et al., 2010; Martin, 1976):

$$\frac{dp_1^*}{dt} = -k \frac{p_1^*}{V_a} \frac{dV_a}{dt} + \frac{p_1^*}{V_a} \frac{k}{\rho_a} \frac{dm_a}{dt} \tag{8}$$

- Air valve characterization (Iglesias-Rey et al., 2014; Wylie & Streeter, 1993): The mass of air flowing through the air valve depends on the value of the atmospheric pressure ($p_{atm}^*$) and the absolute pressure of the air pocket ($p_1^*$).
  - Subsonic air flow in ($p_{atm}^* > p_1^* > 0.528 p_{atm}^*$):

$$Q_{a,nc} = C_{d,adm} A_{adm} \sqrt{7 p_{atm}^* \rho_{a,nc} \left[ \left( \frac{p_1^*}{p_{atm}^*} \right)^{1.4286} - \left( \frac{p_1^*}{p_{atm}^*} \right)^{1.714} \right]} \tag{9}$$

  - Critical air flow in ($p_1^* \leq 0.528 p_{atm}^*$):

$$Q_{a,nc} = C_{d,adm} A_{adm} \frac{0.686}{\sqrt{RT}} p_{atm}^* \tag{10}$$

  where $Q_{a,nc}$ = air flow in normal conditions across the air valve, $C_{d,adm}$ = inflow discharge coefficient, $R$ = air constant, and $T$ = air temperature.

In summary, a 5x5 system of DAE (equations (1), (2), (7), (8), and (9) or (10)) describes the problem. With the corresponding boundary conditions and initial conditions, the solutions to five unknowns can be obtained.

*Initial and boundary conditions*

The initial conditions are described by $v_w(0) = 0$, $L_{e,0} = L_T - x_0$, $p^*_{1,0} = p^*_{atm} = 101325$ Pa, $\rho_{a,0} = 1.205$ kgm$^{-3}$, and $v_{a,nc}(0) = 0$. The boundary conditions are the same as in Case No. 1.

## 3 Model verification

The proposed model was applied to a methacrylate pipeline with an internal diameter of 42 mm and length of 4.36 m. Experiments were conducted at the Fluids Laboratory at the Universitat Politècnica de València (Valencia, Spain). The installation had a water supply tower, a 4.16-m-long methacrylate pipe, a 0.2-m-long PVC pipe, PVC joints, two ball valves with internal diameters of 42 mm at the ends, and a free-surface basement reservoir to collect drainage water. The methacrylate pipeline was first filled, and the emptying process was initiated by opening a ball valve. A transducer was installed upstream to measure the air pocket pressure. Figure 3 shows the experimental setup.

The gravity term for this schematic configuration (see Fig. 3) depends on the position of the emptying column. There are two possibilities:

(1) When the air-water front in the emptying column has not reached the PVC pipe ($L_e >= L_p$):

$$\frac{\Delta z_1}{L_e} = \frac{L_e - L_p}{L_e}\sin(\theta) + \frac{L_p}{L_e}\cos(\theta) \tag{11}$$

(2) When the air-water front in the emptying column has reached the PVC pipe ($L_e < L_p$):

$$\frac{\Delta z_1}{L_e} = \cos(\theta) \tag{12}$$

To verify the proposed model, the computed and measured pressure oscillation patterns and trough pressures were compared. A friction factor of $f = 0.018$ was used based on experimental results. The experiments were carried out using various sizes of the air pocket ($x_0$), pipe slopes ($\theta$), resistance coefficients ($R_v$), and valve maneuvering times ($T_m$). The opening of the ball valve was modeled using a synthetic maneuver with a resistance coefficient.

The results were obtained in both cases using an adiabatic process ($k = 1.4$), which indicates that the experiments are presented as fast transient phenomena. A total of 12 tests were performed for Case No. 1 (see Table 1), while 24 tests were performed for Case No. 2 (12 with $D_{av} = 1.5$ mm and 12 with $D_{av} = 3.0$ mm). Each measurement was repeated twice to confirm the result.

For Case No. 1, the ball valve located upstream was closed before the start of the simulation. Table 1 presents the characteristics of tests 1 through 12 for Case No. 1.

Figure 4 shows oscillations in the first three seconds of tests 7 and 10. The proposed model can predict the pressure oscillation patterns and the associated subatmospheric pressure troughs. Test 7 is characterized by a few waves in the first three seconds, which are produced by opening the ball valve ($R_v = 14.79 \bullet 10^6$ ms$^2$m$^{-6}$), as shown in Fig. 4a. The influence of the valve maneuvering time can be observed in the lag in the pressure oscillation pattern between repetitions 1 and 2, where the minimum subatmospheric pressure head of 8.06 m occurs. Test 10 has a few waves during the transient behavior (see Fig. 4b) and a high flow resistance coefficient value ($R_v = 135.21 \bullet 10^6$ ms$^2$m$^{-6}$), where the trough of 8.14 m occurs in the subatmospheric pressure head.

In Case No. 2, an orifice is established upstream to represent the air valve (Fig. 3b). Two different orifice sizes are used to show the impact of the air inlet. The smallest orifice size corresponds to the lowest value of the inflow discharge coefficient. The inflow discharge coefficients for $D_{av} = 1.5$ mm and $D_{av} = 3.0$ mm are 0.55 and 0.65, respectively. These values were calibrated. Figure 5 shows the

experimental results and characteristic curves for the two orifice sizes. The air flow was measured in the permanent air flow facility at the Thermodynamic Laboratory at the Universitat Politècnica de València (Valencia, Spain), which has a compressor and a maximum capacity of 900 $m^3h^{-1}$, 4 parallel pipes to measure different flows, regulating valves, and transducers to record experimental quantities (air flow in discharges, absolute pressures, and temperatures). The formulation presented by Wylie and Streeter (1993) (equation (9)) predicts the experimental data. Table 2 shows the two selected tests.

Figure 6 shows a comparison between the computed and measured absolute pressure oscillation patterns for tests 13 and 14. Again, the proposed model shows fairly good overall agreement with the experiments. The subatmospheric pressure trough occurs immediately when the ball valve is opened. The absolute pressure starts to increase slowly until it reaches atmospheric conditions. The trough of the subatmospheric pressure head for test 13 (8.92 m) is lower than that of test 14 (9.51 m). Furthermore, test 13 shows a longer transient than test 14.

Figure 7 compares the calculated and measured subatmospheric pressure troughs for both cases. For all tests, the proposed model predicts the trough of the subatmospheric pressure, which ensures the safety of the pipeline. The main risk is presented in Case No. 1, when there is no air inlet near the orifices (air valves). Case No. 2 shows that an orifice of size of $D_{av} = 1.5$ mm results in a greater subatmospheric pressure trough than an orifice of size of $D_{av} = 3.0$ mm.

## 4 Case study and results

To demonstrate the practicality of the model and to quantify the order of magnitude of some terms used, a practical application for Case No. 2 is presented. The system in Fig. 1b is solved with the following parameters: $L_T = 600$ m, $f = 0.018$, $D = 0.35$ m; $\Delta z_0 = 15$ m, $R_v = 0.06$ $ms^2m^{-6}$, $x_0 = 200$ m, $k = 1.2$, $p^*_{1,0} = 101325$ Pa, $D_{av} = 50$ mm ($A_{adm} = 0.0019$ $m^2$), and $C_{d,adm} = 0.50$. The results are also shown in Fig. 8.

From the results, it can be deduced that the maximum water flow of 0.27 $m^3s^{-1}$ in the transient event occurs at 29.5 s, as shown in Fig. 8a. At the beginning of the transient event, there is less air flow than water flow because the valve restricts the air flow rate. At 125.2 s, the air flow surpasses the water flow because a large part of the column length has been drained, which corresponds to a decrease in the output water flow. From 125.2 to 291.2 s, water flow oscillations occur because the water flow rate is now less than the air flow rate (see Fig. 8a). Figure 8b shows that the emptying column is drained completely in 291.2 s. During the first 125.2 s, the length of the emptying column decreases because the water flow is greater than the air flow admitted by the air valve. When oscillations occur in the water flow, the pipe drains more slowly.

The change in absolute pressure parallels the air density in the air pocket (see Fig. 8c). In the beginning, the pressure and density decrease until they reach minimum values of 8.19 m and 0.99 $kgm^{-3}$, respectively, which occur at 86.65 s. These variables increase until they reach atmospheric conditions. Figure 8d presents the components of total energy per unit weight (or total head). The velocity head, potential head, and absolute pressure head are based on Fig. 8a, Fig. 8b, and Fig. 8c, respectively. The total head starts with a value of 20.33 m, where the water velocity is null, the air pocket is at atmospheric conditions (101325 Pa), and the initial potential head is 10.0 m. The velocity head has no relevance during the hydraulic event. The total head is the sum of the absolute pressure head and the potential head. The total head decreases from 0 to 150 s. From 150 to 291.2 s, the total head decreases slowly with values close to atmospheric conditions (101325 Pa or 10.33 m).

## 5 Conclusions

Emptying processes have received little attention from researchers. However, the development of models to simulate transient behavior in these processes is considered to be of great interest to the scientific community. In this work, a mathematical model was developed for analyzing the transient phenomena during the emptying process of a single pipe. The proposed model was validated using an experimental setup. The computed and measured absolute pressure oscillation patterns were compared, which showed that the proposed model accurately depicts the experimental phenomena. The proposed model can predict the subatmospheric pressure pattern, which is important for pipe stiffness and air valve selection.

Finally, the proposed model was applied in a theoretical case to quantify the order of magnitude of the main hydraulic variables. Based on the analysis, the following conclusions can be drawn:

- Without air valves (Case No. 1), troughs of subatmospheric pressure are generated, which could cause a collapse of the system. The total length of the emptying column will not completely drain. To avoid these problems, air valves must be installed at the high points of the installation (Case No. 2). If the size of the air valve is suitable (i.e., well designed), the pipe displays a small trough of subatmospheric pressure. If the size is inappropriate, the amount of air required does not enter the system, and significant troughs of subatmospheric pressure can be reached. As a consequence, the system could collapse.
- It is recommended that great care be taken during the emptying process when an entrapped air pocket is present in the system. Slow maneuvers of the ball valve are recommended to admit the air required into the system through the air valve.

The next step is to analyze more complex systems to expand the research on this topic, such as pipelines with an irregular profile, with several pipes, several air pockets, various valves, and various air valves.

## 6 Acknowledgements

This work was supported by the Fundación CEIBA - Gobernación de Bolívar, Colombia. This study was also supported by the Program Initiation into Research (Project 11140128) of the Comisión Nacional de Investigación Científica y Tecnológica (Conicyt), Chile.

## Notation

$A$ = cross-sectional area of pipe ($m^2$)
$A_{adm}$ = cross-sectional area of the air valve ($m^2$)
$C_{d,adm}$ = inflow discharge coefficient (–)
$D$ = internal pipe diameter (m)
$D_{av}$ = air valve diameter or orifice size (mm)
$f$ = Darcy-Weisbach friction factor (–)
$g$ = gravity acceleration ($ms^{-2}$)
$H$ = energy per unit weigh (m)
$h_m$ = minor losses (m)
$L_e$ = length of emptying column (m)
$L_T$ = pipe length (m)
$k$ = polytrophic coefficient (–)
$m$ = mass (kg)
$p_1$ = pressure of air pocket (Pa)
$p_{atm}$ = atmospheric pressure (Pa)
$Q$ = discharge ($m^3s^{-1}$)
$R$ = air constant (287 $Jkg^{-1}{}^{\circ}K^{-1}$)
$R_v$ = resistance coefficient ($ms^2m^{-6}$)
$t$ = time (s)
$T$ = air temperature (°K)
$T_m$ = valve maneuvering time (s)
$v$ = velocity ($ms^{-1}$)
$V$ = volume ($m^3$)
$x$ = length of entrapped air pocket (m)
$z$ = elevation of pipe (m)
$\Delta z_1$ = elevation difference (m)
$\rho$ = density ($kgm^{-3}$)
$\gamma$ = unit weight ($Nm^{-3}$)

*Superscripts*
$^*$ = absolute values (e.g., absolute pressure)

*Subscripts*
0 = initial condition (e.g., initial length of emptying column)
$a$ = refers to air (e.g., air density)
$w$ = refers to water (e.g., water density)
$nc$ = normal conditions

## References

Bashiri-Atrabi, H., & Hosoda, T. (2015). The motion of entrapped air cavities in inclined ducts. *Journal of Hydraulic Research*, *53*(6), 814–819.

Cabrera, E., Abreu, J., Pérez, R., & Vela, A. (1992). Influence of liquid length variation in hydraulic transients. *Journal of Hydraulic Research*, *118*(12), 1639–1650.

Coronado-Hernández, O. E., Fuertes-Miquel, V. S., Iglesis-Rey, P. L., & Martínez-Solano, F. J. (2018). Rigid water column model for simulating the emptying process in a pipeline using pressurized air. *Journal of Hydraulic Engineering*, *144*(4).

Fuertes, V. (2001). *Hydraulic transients with entrapped air pockets* (Unpublished doctoral dissertation). Department of Hydraulic Engineering, Polytechnic University of Valencia, Spain.

Fuertes-Miquel, V. S., López-Jiménez, P. A., Martínez-Solano, F. J., & López-Patiño, G. (2016). Numerical modelling of pipelines with air pockets and air valves. *Canadian Journal of Civil Engineering*, *43*(12), 1052–1061.

Guinot, V. (2001). The discontinuous profile method for simulating two-phase flow in pipes using the single component approximation. *International Journal for Numerical Methods in Fluids*, *37*(3), 341–359.

Hou, Q., Tijsseling, A., Laanearu, J., Annus, I., Koppel, T., Bergant, A., ... Van't Westende, J. (2014). Experimental investigation on rapid filling of a large-scale pipeline. *Journal of Hydraulic Engineering*, *140*(11).

Iglesias-Rey, P. L., Fuertes-Miquel, V. S., García-Mares, F. J., & Martínez-Solano, F. J. (2014). Comparative study of intake and exhaust air flows of different commercial air valves. In *16th conference on water distribution system analysis,* WDSA 2014 (pp. 1412–1419).

Izquierdo, J., Fuertes, V., Cabrera, E., Iglesias, P., & Garcia-Serra, J. (1999). Pipeline start-up with entrapped air. *Journal of Hydraulic Research*, *37*(5), 579–590.

Laanearu, J., Annus, I., Koppel, T., Bergant, A., Vučković, S., Hou, Q., ... Van't Westende, J. (2012). Emptying of large-scale pipeline by pressurized air. *Journal of Hydraulic Engineering*, *138*(12), 1090–1100.

Lee, N. (2005). *Effect of pressurization and expulsion of entrapped air in pipelines* (Unpublished doctoral dissertation). School of Civil and Environmental Engineering, Georgia Institute of Technology, United States.

Leon, A., Ghidaoui, M., Schmidt, A., & Garcia, M. (2010). A robust two-equation model for transient-mixed flows. *Journal of Hydraulic Research*, *48*(1), 44–56.

Liou, C., & Hunt, W. (1996). Filling of pipelines with undulating elevation profiles. *Journal of Hydraulic Engineering*, *122*(10), 534–539.

Liu, D., Zhou, L., Karney, B., Zhang, Q., & Ou, C. (2011). Rigid-plug elastic water model for transient pipe flow with entrapped air pocket. *Journal of Hydraulic Research*, *49*(6), 799–803.

Malekpour, A., & Karney, B. (2014). Column separation and rejoinder during rapid pipeline filling induced by a partial flow blockage. *Journal of Hydraulic Research*, *52*(5), 693–704.

Martin, C. (1976). Entrapped air in pipelines. In *Proc. of the second international conference on pressure surges.* London, England.

Martins, S. C., Ramos, H. M., & Almeida, A. B. (2010). Mathematical modeling of pressurized system behaviour with entrapped air. In *Environmental hydraulics: Theoretical, experimental and computational solutions* (pp. 61–64).

Martins, S. C., Ramos, H. M., & Almeida, A. B. (2015). Conceptual analogy for modelling entrapped air action in hydraulic systems. *Journal of Hydraulic Research*, *53*(5), 678–686.

Pozos, O., González, C., Giesecke, J., Marx, W., & Rodal, E. (2010). Air entrapped in gravity pipeline systems. *Journal of Hydraulic Research*, *48*(3), 338–347.

Tijsseling, A., Hou, Q., Bozkuş, Z., & Laanearu, J. (2016). Improved one-dimensional models for rapid emptying and filling of pipelines. *Journal of Pressure Vessel Technology*, *138*(3), 031301.

Wang, H., Zhou, L., Liu, D., Karney, B., Wang, P., Xia, L., ... Xu, C. (2016). *CFD* approach for column separation in water pipelines. *Journal of Hydraulic Engineering*, *142*(10).

Wang, K., Shen, Q., & Zhang, B. (2003). Modeling propagation of pressure surges with the formation of an air pocket in pipelines. *Computers & Fluids*, *32*(9), 1179–1194.

Wylie, E., & Streeter, V. (1993). *Fluid transients in systems.* New Jersey, NJ: Ed. Prentice Hall.

Zhou, L., & Liu, D. (2013). Experimental investigation of entrapped air pocket in a partially full water pipe. *Journal of Hydraulic Research*, *51*(4), 469–474.

Zhou, L., Liu, D., & Karney, B. (2013a). Investigation of hydraulic transients of two entrapped air

pockets in a water pipeline. *Journal of Hydraulic Engineering*, *139*(9), 949–959.

Zhou, L., Liu, D., & Karney, B. (2013b). Phenomenon of white mist in pipelines rapidly filling with water with entrapped air pocket. *Journal of Hydraulic Engineering*, *139*(10), 1041–1051.

## List of tables

**List of figures**

Table 1 Case No. 1 - Experimental setup - Characteristics of tests 1 to 12

| Test No. | 1 | 2 | 3 | 4 | 5 | 6 | 7 | 8 | 9 | 10 | 11 | 12 |
|---|---|---|---|---|---|---|---|---|---|---|---|---|
| $x_0$ (m) | 0.205 | 0.340 | 0.450 | 0.205 | 0.340 | 0.450 | 0.205 | 0.340 | 0.450 | 0.205 | 0.340 | 0.450 |
| $\theta$ (rad) | 0.457 | 0.457 | 0.457 | 0.457 | 0.457 | 0.457 | 0.515 | 0.515 | 0.515 | 0.515 | 0.515 | 0.515 |
| $R_v \bullet 10^{-6}(\mathrm{ms^2m^{-6}})$ | 11.89 | 11.89 | 11.89 | 25.00 | 22.68 | 30.86 | 14.79 | 14.79 | 14.79 | 135.21 | 138.41 | 100.00 |
| $T_m$ (s) | 0.40 | 0.40 | 0.50 | 0.25 | 0.15 | 0.30 | 0.50 | 0.40 | 0.75 | 0.30 | 0.30 | 0.30 |

Table 2 Case No. 2 - Experimental setup - Characteristics of tests 13 and 14

| Test No. | $D_{av}$ (mm) | $x_0$ (m) | $\theta$ (rad) | $R_v \bullet 10^{-6}$ ($ms^2m^{-6}$) | $T_m$ (s) |
|---|---|---|---|---|---|
| 13 | 1.5 | 0.340 | 0.515 | 17.36 | 0.40 |
| 14 | 3.0 | 0.340 | 0.515 | 2.60 | 0.35 |

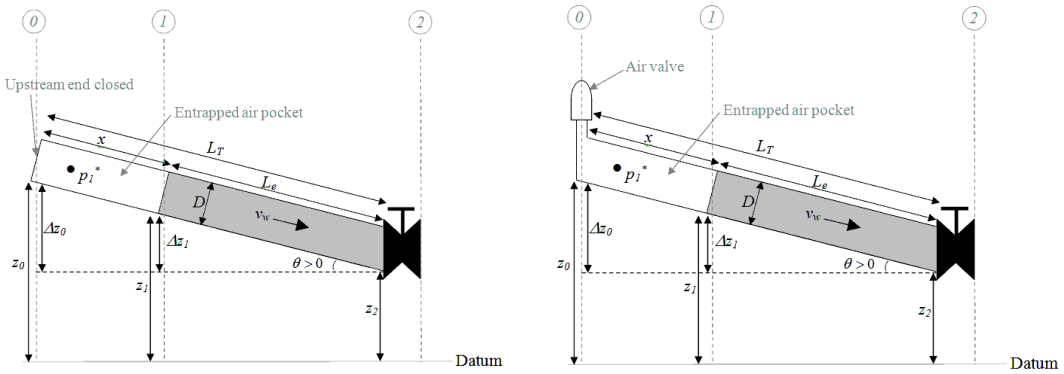


(a) Case No. 1: A simple pipe with the upstream end closed

(b) Case No. 2: A simple pipe with an air valve installed on the upstream end

Figure 1 Schematic of an entrapped air pocket in a single pipe while water empties

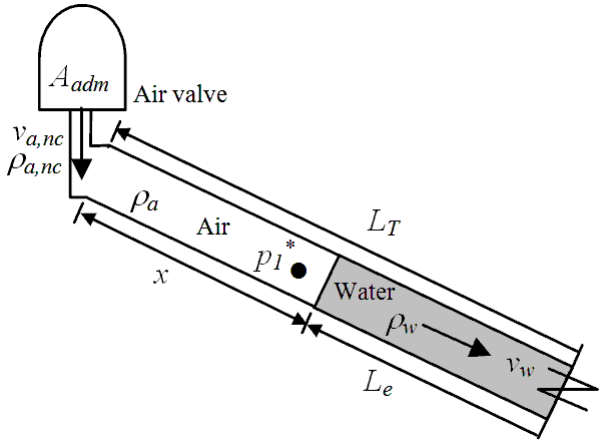


Figure 2 Location of air valve

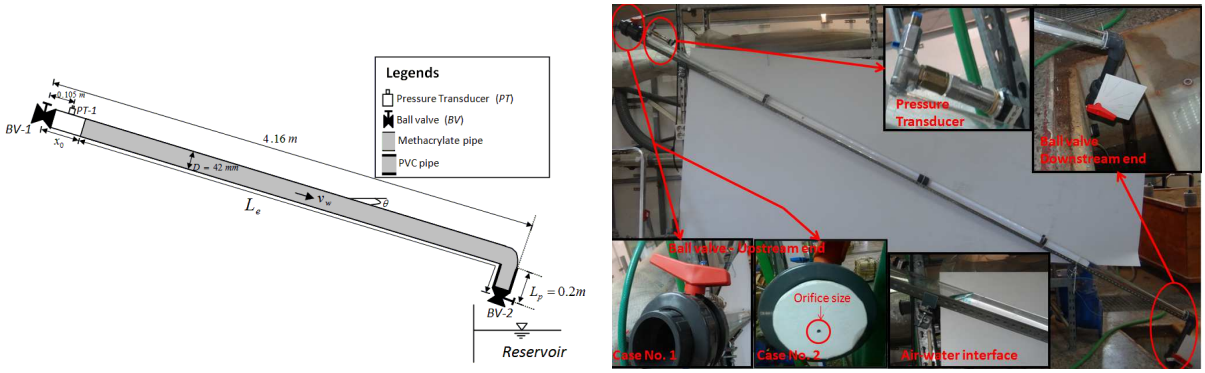


(a) Facility scheme

(b) Details of experimental setup

Figure 3 Schematic of experimental setup

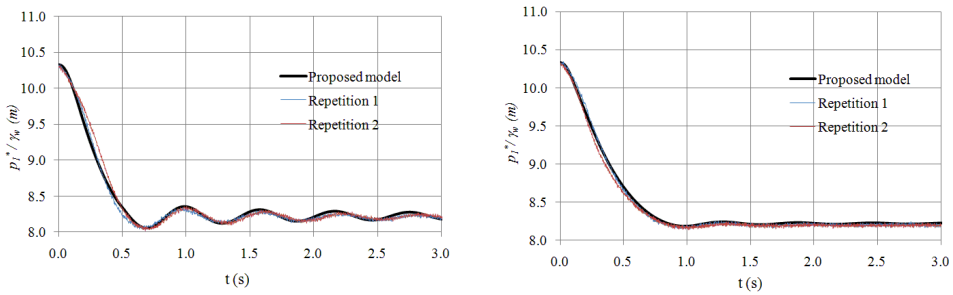


(a) Test 7 (b) Test 10

Figure 4 Case No. 1 - Comparisons between calculated and measured absolute pressures of the air pocket for tests 7 and 10

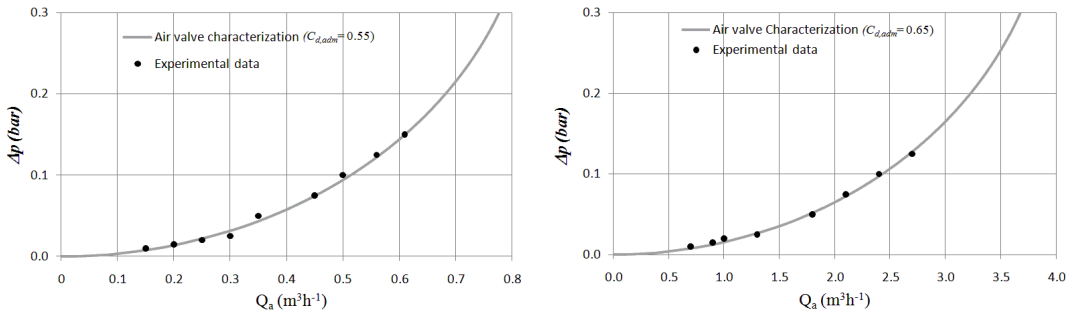


(a) $D_{av} = 1.5$ mm (b) $D_{av} = 3.0$ mm

Figure 5 Laboratory test results of air valves during air admission

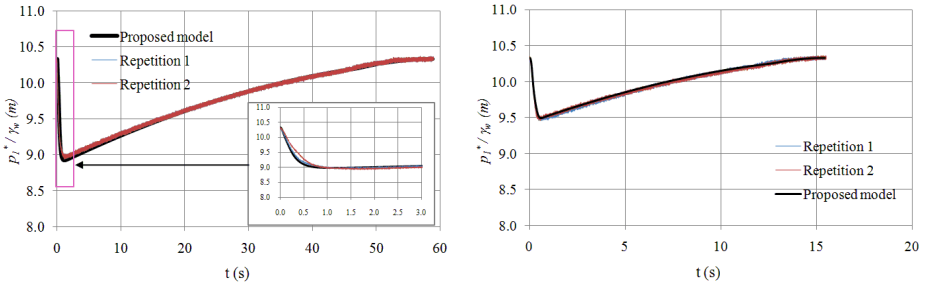


(a) Test 13 (b) Test 14

Figure 6 Case No. 2 - Comparisons between calculated and measured absolute pressure of the air pocket for tests 13 and 14

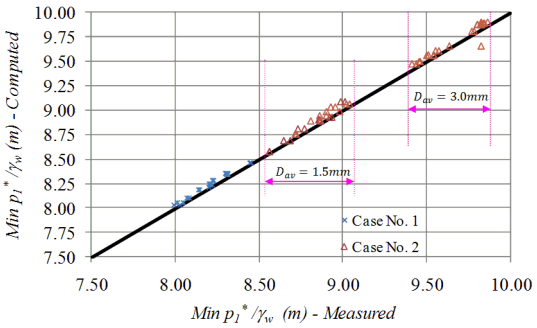


Figure 7 Comparison between computed and measured minimum pressures

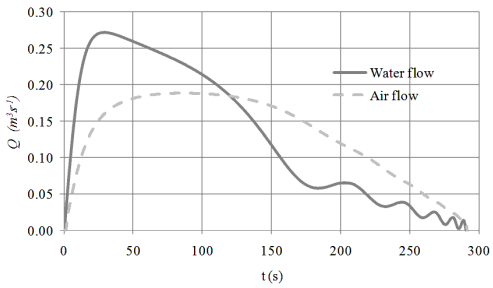


(a) Water and air flow

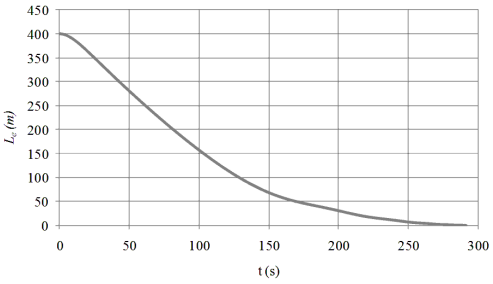


(b) Length of emptying column

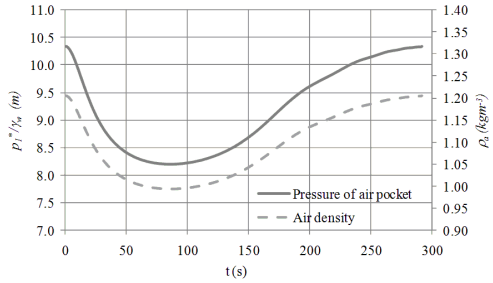


(c) Absolute pressure and density of the air pocket

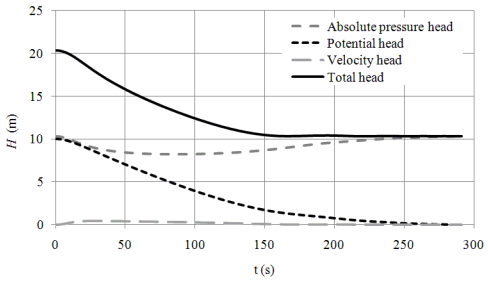


(d) Energy per unit weight

Figure 8 Results of Case Study - Full transient analysis of the system under consideration